Interferon-α-induced cytoplasmic MxA structures in hepatoma Huh7 and primary endothelial cells

Deodate Davis[1], Huijuan Yuan[1], Yang-Ming Yang[1], Feng-Xia Liang[2], Pravin B. Sehgal[1,3]

[1]Department of Cell Biology & Anatomy, New York Medical College, Valhalla, New York, USA
[2]Division of Advanced Research Technologies, New York University School of Medicine, New York, USA
[3]Department of Medicine, New York Medical College, Valhalla, New York, USA

Aim of the study: Interferon (IFN)-α is now established as a treatment modality in various human cancers. The IFN-α-inducible human "myxovirus resistance protein A" (MxA) is a cytoplasmic dynamin-family large GTPase primarily characterized for its broad-spectrum antiviral activity and, more recently, for its anti-tumor and anti-metastasis effects. We characterized the association of IFN-α-induced MxA with cytoplasmic structures in human Huh7 cancer cells and in primary endothelial cells.

Material and methods: We re-evaluated the long-standing inference that MxA associated with the smooth ER using double-label immunofluorescence techniques and the ER structural protein RTN4 as a marker for smooth ER in IFN-α-treated cells. We also evaluated the relationship of exogenously expressed HA-MxA and GFP-MxA with mitochondria, and characterized cytoplasmic GFP-MxA structures using correlated light and electron microscopy (CLEM).

Results and conclusions: We discovered that IFN-α-induced endogenous MxA associated with variably-sized endosome-like and reticular cytoplasmic structures which were distinct from the ER. Thin-section EM studies of GFP-MxA expressing Huh7 cells showed that GFP-MxA formed variably-sized clusters of vesiculotubular elements to form endosome-like "MxA bodies". Many of these clusters stretched out alongside cytoskeletal elements to give the appearance of a cytoplasmic "MxA reticulum". This MxA meshwork was distinct from but adjacent to mitochondria. GFP-MxA expressing Huh7 cells showed reduced MitoTracker uptake and swollen mitochondria by thin-section EM. The new data identify cytoplasmic MxA structures as novel organelles, and suggest cross-talk between MxA structures and mitochondria that might account for the increased anti-tumoral efficacy of IFN-α combined with ligands that activate other pattern-sensing receptor pathways.

Key words: interferons, myxovirus resistance protein A, dynamin-family GTPase, MxA bodies, MxA reticulum, mitochondrial function, correlated light and electron microscopy (CLEM).

Contemp Oncol (Pozn) 2018; 22 (2): 86–94
DOI: https://doi.org/10.5114/wo.2018.76149

Introduction

Type I interferons (IFN-α and -β) are used extensively in the treatment of different types of human cancer, leukemia, viral infections and multiple sclerosis [reviewed in 1–6]. IFN-α therapy has proven especially useful in myeloproliferative neoplasms such as polycythemia vera and myelofibrosis [2–6]. Exposure of cancer cells to IFNs upregulates a large array of genes primarily through the Jak-STAT signaling pathway [2–6]. It has long been established that IFNs decrease cancer cell proliferation, motility and invasiveness [1, 5, 6]. IFN induction in human cells is itself a process which is triggered by multiple pathways including infection with RNA and DNA viruses, foreign nuclei acids, cytosolic self DNA, endogenous dinucleotides and other microbial products utilizing pathways initiated through cytoplasmic pattern recognition receptor molecules which lead to activation of transcription factor cascades (NF-κB activation, IRF3 and IRF7 activation) through mechanisms which include the TLR (cytoplasmic "Toll-like receptors"), STING ("stimulator of interferon genes" protein which is associated with the endoplasmic reticulum) and MAVS (mitochondrial antiviral signaling protein associated with mitochondria) pathways [1, 7–12]. Moreover, the combination of IFN-α with ligands such as poly(I).poly(C) (e.g. Ampligen) which activate the Toll-like receptor (TLR) pathways (e.g. TLR3 activation by poly(I).poly(C)/Ampligen) is attracting increasing attention in cancer immunotherapy [13]. Thus, inter-organellar communication and cross-talk is a critical aspect of these signaling interactions which synergize to enhance anti-tumoral efficacy [7–13].

It was discovered beginning several decades ago that the "myxovirus resistance protein A" (MxA) was markedly (50–200-fold) induced when cells were exposed to Type I (α and β) and Type III (λ) but not Type II (γ) IFNs [14–16]. Human MxA is a ~70 kDa dynamin-family large GTPase with membrane association activity [14–16]. In cell-free systems, MxA oligomerizes into dimers, tetramers and higher-order structures and tubulates lipid membranes [14–16]. Mushinski et al. discovered that exogenously expressed wt MxA inhibited the motility and invasiveness of PC3M prostate cancer cells, including hepatic metastasis [17]. Indeed, deletion of MxA was inversely associated with prostate cancer and MxA regulated cell cycle, invasiveness and docetaxel-induced apoptosis [18]. MxA often shows single amino acid mutations in a variety of cancers [19]. More recently, working in human Huh7 hepatoma cells, Shi et al. observed that transient exogenous expression of MxA reduced hepatitis C virus replication, stimulated IFN-α and β production, upregulated IRF3, IRF7, TRIF, MDA-5, ISG15, ISG12a, and also activated pSTAT1 [20]. Since these represent signature consequences of activation of the STING pathway [7–12], the data of Shi et al. [20] suggested to us that MxA might cross-talk with the STING pathway located in the ER.

We confirmed the strong IFN-α-inducibility of MxA in primary human pulmonary arterial endothelial cells (HPAECs) by Western blotting assays [21]. In these cells, the transient transfection of an expression vector for HA-MxA led to the appearance of punctate endosome-like HA-MxA structures that lined up alongside microtubules, carried markers corresponding to early endosomes (clathrin light chain, early endosomal antigen 1, and Rab5) but were distinct from tubules of the standard endoplasmic reticulum (ER) (immunolabelled by reticulon-4, RTN4) [21–23] (contrary to reports in the previous literature which associated MxA with the ER [14–16, 24]). More recently we observed that the transient transfection of HA-MxA or GFP-MxA vectors into human hepatoma Huh7 cells led to the development of MxA in motile cytoplasmic endosome-like structures as well as, in some cells, an extensive filamentous MxA network distinct from the standard RTN4-based ER [21–23]. In the present study we provide further evidence showing that IFN-α-induced endogenous MxA in human Huh7 hepatoma cells and in primary human endothelial cells associated with cytoplasmic structures distinct from the standard RTN4-based ER. Moreover, we observed that Huh7 cells expressing GFP-MxA showed reduced mitochondrial function and swollen mitochondria. Thin-section electron microscopy (EM) data from correlated light and EM (CLEM) studies helped identify the structure of cytoplasmic EM endosome-like "bodies" in Huh7 cells as clusters of vesiculo-tubular elements without an enveloping membrane. Many of these associated with cytoskeletal elements giving rise to a distinctive criss-cross reticular pattern. The new data provide a basis for exploring functional cross-talk between the MxA cytoplasmic structures and mitochondria in cancer cells.

Material and methods

Cells and cell culture

Human hepatoma cell line Huh7 [25] was a gift from Dr. Charles M. Rice, The Rockefeller University. Huh7 cells were grown in DMEM supplemented with 10% v/v fetal bovine serum (FBS) in 90 mm plates or T-25 flasks. For experiments Huh7 cells were grown in regular 6-well plates or in 35 mm dishes. Primary human pulmonary arterial endothelial cells (HPAECs) were purchased from Clonetics (San Diego, CA) [21]. These were seeded into T-25, T-75 or 6-well plates coated with fibronectin, collagen and bovine serum albumin (respectively 1 µg/ml, 30 µg/ml and 10 µg/ml in coating medium) [21]. HPAECs were grown in Medium 200 supplemented with low serum growth supplement LSGS (Cascade Biologics, Carlsbad, CA) and were used between passages 4 and 10. For CLEM, Huh7 cells were grown sparsely in 35 mm gridded 1.5 mm coverslip plates (Cat. No. P35G-1.5-14-C-GRID; MatTek Corporation, Ashland, MA). Recombinant human IFN-α2a was purchased from BioVision (Milpitas, CA). In the present experiments Huh7 cultures were exposed for two days to IFN-α at a concentration of 3,000 IU/ml prior in DMEM supplemented with 2% FBS prior to fixation and immunofluorescence analyses [21].

Plasmids and transient transfection

The HA-tagged human MxA expression vector (cloned into a pcDNA3 vector) was a gift from Dr. Otto Haller (University of Freiburg, Germany) [24], while the GFP (1-248)-tagged human MxA expression vector was a gift of Dr. Jovan Pavlovic (University of Zurich, Switzerland) [26, 27]; Transient transfections were carried out using just subconfluent cultures in 35 mm plates or in wells of a 6-well plate using DNA in the range of 0.3–2 µg/culture and the Polyfect reagent (Qiagen, Germantown, MD) and the manufacturer's protocol.

Cell extracts and Western blotting

Whole cell extracts were prepared from Huh7 cells as described previously [21 and citations therein]. Western blotting was carried out using 10% SDS-polyacrylamide gels under reducing denaturing conditions as per procedures and protocols provided by Cell Signaling Technology Inc. and ECL detection kit purchased from Thermo Scientific (34077) (Rockford, IL) and Michigan Diagnostics (FWPD02-25) (Royal Oak, MI). Multiple exposures of each blot were obtained to ensure that each of the signals was within the linear range. Western blot signals were quantitated using a Hoefer Scientific GS-300 scanning densitometer. Images in blots were quantitated for optical density also using the NIH Image J software.

Immunofluorescence imaging

Typically, 2 days after IFN-α treatment or 1–2 days after transient transfection of respective vectors, the cultures were fixed using cold paraformaldehyde (4%) for 1 hour and then permeabilized using a buffer containing digitonin (50 µg/ml)/sucrose (0.3M) [21]. Single-label and double-label immunofluorescence assays were carried out using antibodies described previously [21]. Fluorescence was imaged as previously reported [21] using an erect Zeiss AxioImager M2 motorized microscopy system with Zeiss W N-Achroplan 40X/NA0.75 water immersion or Zeiss EC Plan-Neofluor 100X/NA1.3 oil objectives equipped with an high-resolution RGB HRc AxioCam camera and AxioVision 4.8.1 software in a 1388 × 1040 pixel high speed color capture mode. Deconvolution of 2-D images was carried out using Image J (Fiji) software. All data within each experiment were collected at identical imaging settings. Colocalization analyses were carried out using Image J software (Fiji) and deriving the Pearson's colocalization coefficient *R* with Costes' automatic thresholding [28] (*R* = 1.0 for complete colocalization and *R* = 0.0 for complete separation; typically, *R* should be > 0.8 for a "positive" colocalization result [21-23]). Line scans were carried out using AxioVision 4.8.1 software.

MitoTracker uptake

Huh7 cultures transfected with the GFP-MxA vector were exposed to MitoTracker Red CMXRos (Invitrogen, OR) (5 nM for 15 min in growth medium), washed with PBS and imaged in both green (for GFP) and red (for MitoTracker) at fixed exposure settings for each color channel. MitoTracker

uptake in GFP-positive and GFP-negative cells was quantitated using Image J software.

Electron microscopy

For CLEM, Huh7 cells plated sparsely in 35 mm gridded coverslip plates were transiently transfected with the pGFP-MxA vector. Three days later the cultures were fixed with 4% paraformaldehyde for 1 hour at 4°. Confocal imaging was carried out using a tiling protocol to identify the location of specific cells with GFP-MxA structures on the marked coverslip grid. The cultures were then further fixed (2.5% glutaraldehyde for 2 hours at 4°C, post-fixed with 1% osmium tetroxide for 1.5 hours at room temperature), and embedded (in Araldite 502; Electron Microscopy Sciences, Hatfield, PA). The previously identified grid locations of GFP-positive cells were used for serial thin-sectioning (60 nm), mounted on formvar/carbon-ciated slot copper grids and stained with uranyl acetate and lead citrate using standard methods. Stained grids were examined using a Philips CM-12 electron microscope (FEI; Eindhoven, The Netherlands) and images photographed with using a Gatan (4K × 2.7K) digital camera (Gatan, Inc., Pleasanton, CA) [21]. The tiled light microscopy data were correlated with the tiled EM thin-section data to identify GFP-positive cells and fluorescent structures.

Antibody reagents

Rabbit pAb to human MxA (also referred to as human Mx1) (H-285) (sc-50509), goat pAb to RTN4/NogoB (N18) (sc-11027) and mouse mAbs to β-tubulin (2-28-33) (sc-23949) were purchased from Santa Cruz Biotechnology Inc. (Santa Cruz, CA). Mouse mAb to the HA tag (262K, #2362) was purchased from Cell Signaling (Dancers, MA). Respective AlexaFluor 488- and AlexaFluor 594-tagged secondary donkey antibodies to rabbit (A-11008 and A-11012), mouse (A-21202 and A-21203) or goat (A-11055 and A-11058) IgG were from Invitrogen Molecular Probes (Eugene, OR).

Results

IFN-α-induced endogenous MxA in Huh7 cells localized to cytoplasmic structures distinct from the standard RTN4-ER

In contrast to the previous report by Stertz *et al.* [24], the data in Figs. 1 and 2 show that IFN-α-induced endogenous MxA in Huh7 cells was observed in filamentous and endosome-like cytoplasmic structures that were distinct from the standard RTN4-based ER. Figures 1A and 1B confirm the marked (> 40-fold) inducibility of MxA in Huh7 cells upon exposure to IFN-α in our hands. Figure 1C shows that the MxA was localized manly in the cytoplasm in reticular filamentous structures. The high magnification imaging of MxA and RTN4 structures in the cytoplasm as in Fig. 1D showed that the MxA and RTN4 structures were distinct (the correlation coefficient *R* was only 0.14). The line scan shown in Fig. 1E through the cytoplasm reveals clearly that MxA and RTN4 did not co-localize.

High magnification imaging at the cell periphery is summarized in Figs. 2A and 2B to highlight the observation of RTN4 in discrete ER tubules, and that the endogenous MxA was in structures distinct from these smooth ER tubules (the correlation coefficient *R* was only 0.16 and 0.23 respectively). The line scans in Figs. 2C and 2D further emphasize the marked disparity between the structures containing MxA and those corresponding to the standard RTN4-positive ER tubules.

Localization of IFN-α-induced endogenous MxA in primary endothelial cells to diverse cytoplasmic structures all distinct from the RTN4-ER

We have reported earlier that IFN-α strongly induced endogenous MxA in HPAECs when cell extracts were assayed using Western blots [21]. In the present study we evaluated the localization of this endogenous MxA in the cytoplasm and compared that to the distribution of RTN4-based ER (Figs. 3 and 4). Figure 3A shows the distribution MxA in the HPAEC cytoplasm in structures that are distinct from RTN4. The line scan in Fig. 3B confirms this disparity (arrow). The data in Figs. 4A and 4C (and respective line scans in Figs. 4B and 4D, arrows) not only confirm this disparity in additional HPAECs but also illustrate the localization of endogenous MxA to the plasma membrane in Fig. 4A and in larger globular cytoplasmic structures in Fig. 4B.

Taken together, the data in Figs. 1–4 show that endogenous IFN-α-induced MxA localized in different cytoplasmic structures none of which corresponded to the standard RTN4-based ER in contrast to what has been claimed in the previous MxA literature [14–16, 24 and citations therein]. The present data pertaining to endogenous MxA are consistent with our previous observations that HA-MxA and GFP-MxA derived from transfected expression vectors also did not co-localize with the RTN4-based ER [21–23].

Reduction of mitochondrial function in MxA expressing Huh7 cells

We investigated the association of MxA with mitochondria and also the potential influence of MxA on mitochondrial function in Huh7 cells. Figure 5A summarizes representative images of an Huh7 cell expressing HA-MxA overlapped with F1-ATPase immunostaining for mitochondria. The HA-MxA formed a cytoplasmic reticulum which was distinct from but was located close to mitochondria. Furthermore, Figure 5B summarizes data showing that the level of MitoTracker uptake was distinctly reduced in Huh7 cells expressing MxA. Thus, the expression of exogenous MxA appeared to have compromised mitochondrial function.

Thin-section EM of GFP-MxA bodies using the CLEM approach

In order to characterize the cytoplasmic structures in Huh7 cells corresponding to the MxA endosome-like "bodies" we transfected Huh7 cells with the GFP-MxA vector and carried out CLEM. Figure 6A illustrates a representative result. The cytoplasm of GFP-MxA expressing cells contained GFP-MxA structures (arrows in Fig. 6A) which consisted of clusters of vesiculo-tubular structures of size 90–200 nm clustered into variably sized "bodies" lacking an enveloping membrane. Many of these GFP-MxA bodies

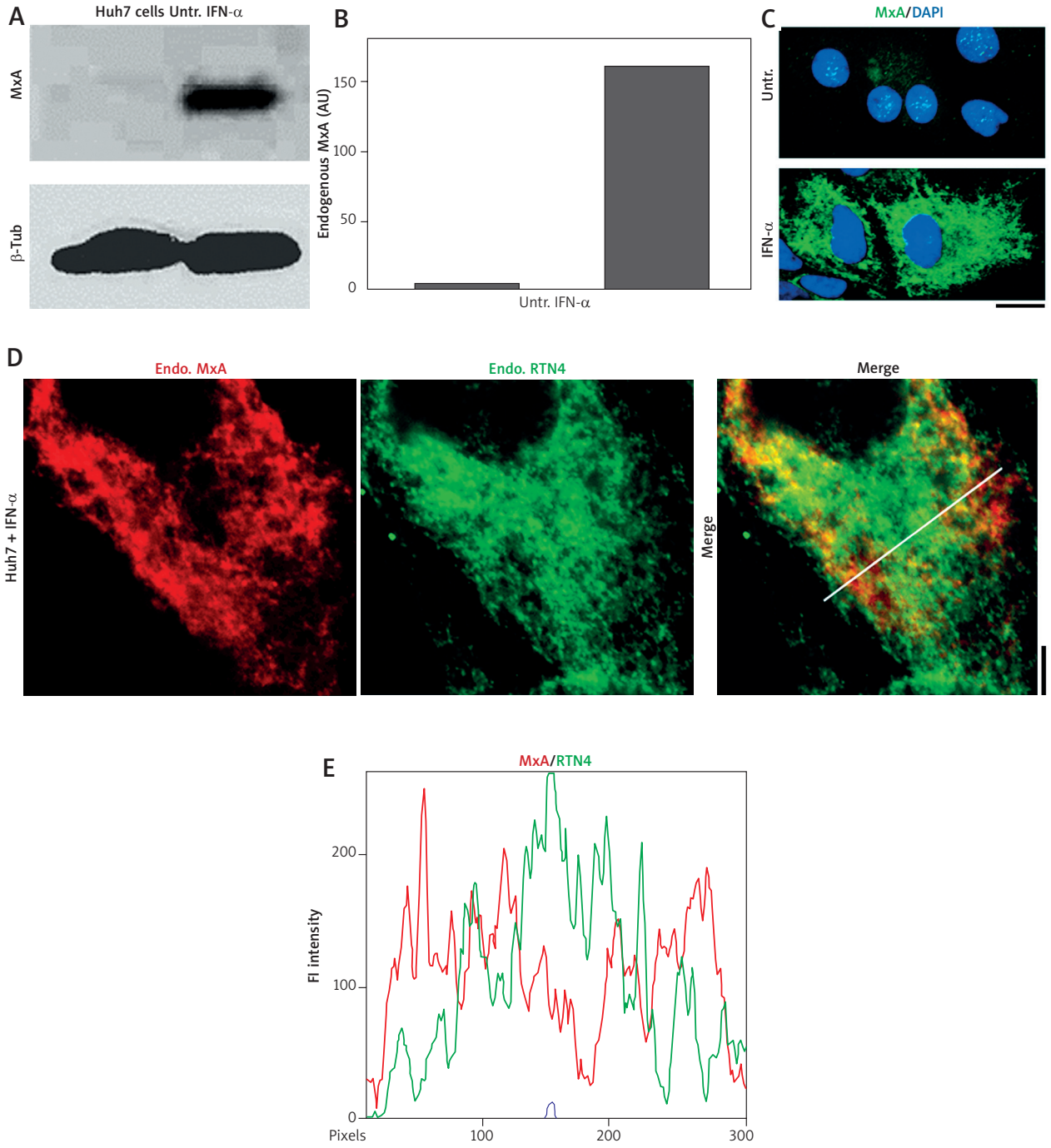

Fig. 1. IFN-α-induced endogenous MxA in cytoplasm of Huh7 cells associated with structures distinct from the RTN4-based standard ER. Replicate cultures of Huh7 cells in 35 mm plates were exposed to recombinant IFN-α2a (3,000 IU/ml) in DMEM supplemented with 2% fetal bovine serum ("low-serum medium") for 2 days or left untreated (Untr). Respective cultures were processed for preparing total cell extract or for double-label immunofluorescence imaging as indicated. Panels A and B, Western blots showing strong expression induction of MxA in Huh7 cells and quantitation (estimate: ~40-fold induction in this experiment). In the Western blots, β-tubulin was used as a loading control. Panel C, immunofluorescence images showing IFN-stimulated expression of endogenous MxA in the cytoplasm of Huh7 cells in a reticular pattern (25-35% of cells showed this pattern) imaged using a 40 × water-immersion objective. Scale bar = 10 µm. Panel D, Double-label immunofluorescence analyses of IFN-treated Huh7 cells for MxA and RTN4 imaged using an 100× oil immersion objective. Scale bar = 5 µm. The white line in the merged image in this panel indicates region depicted in the line scan in Panel E. *R* value indicated in the merged image in Panel D corresponds to the respective Pearson's R coefficients (after automatic Costes' thresholding) (co-localization corresponds to $R > 0.8$ [28])

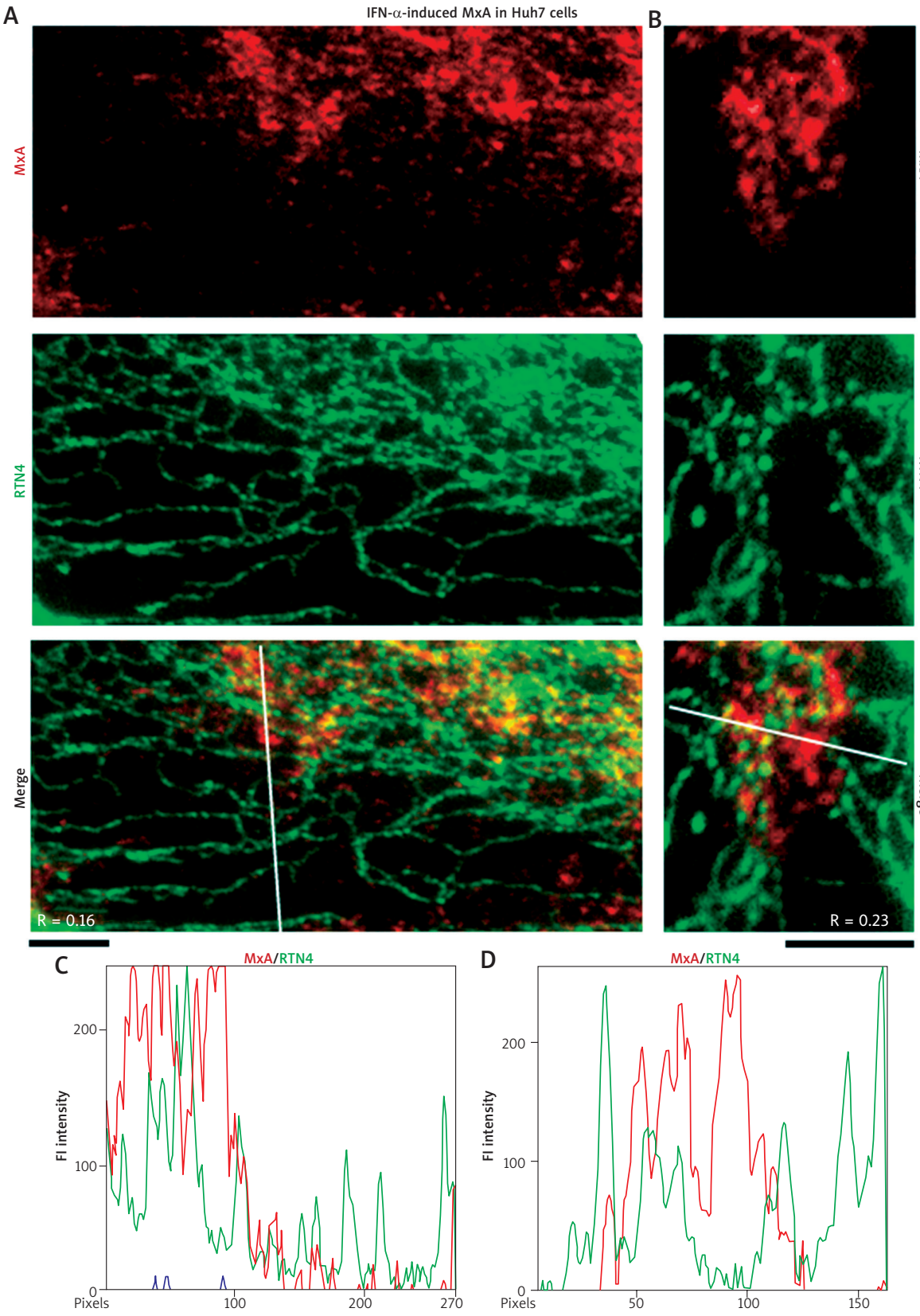

Fig. 2. IFN-α-induced endogenous MxA in cytoplasm of Huh7 cells associated with structures distinct from RTN4 tubules of the standard ER. Replicate cultures of Huh7 cells in 35 mm plates were exposed to recombinant IFN-α2a (3,000 IU/ml) in DMEM supplemented with 2% fetal bovine serum ("low-serum medium") for 2 days or left untreated (Untr) (as in Fig. 1), fixed and processed for double-label immunofluorescence imaging by sequentially probing for RTN4 first (in green) and then endogenous MxA (in red). The cells were imaged using an 100x oil immersion objective. Panels A and B represent two independent experiments. Scale bars = 5 µm. *R* values indicated in the merged images in Panels A and B correspond to the respective Pearson's R coefficients (after automatic Costes' thresholding). White lines in the merged images in Panels A and B indicate regions depicted in the line scans in Panels C and D respectively

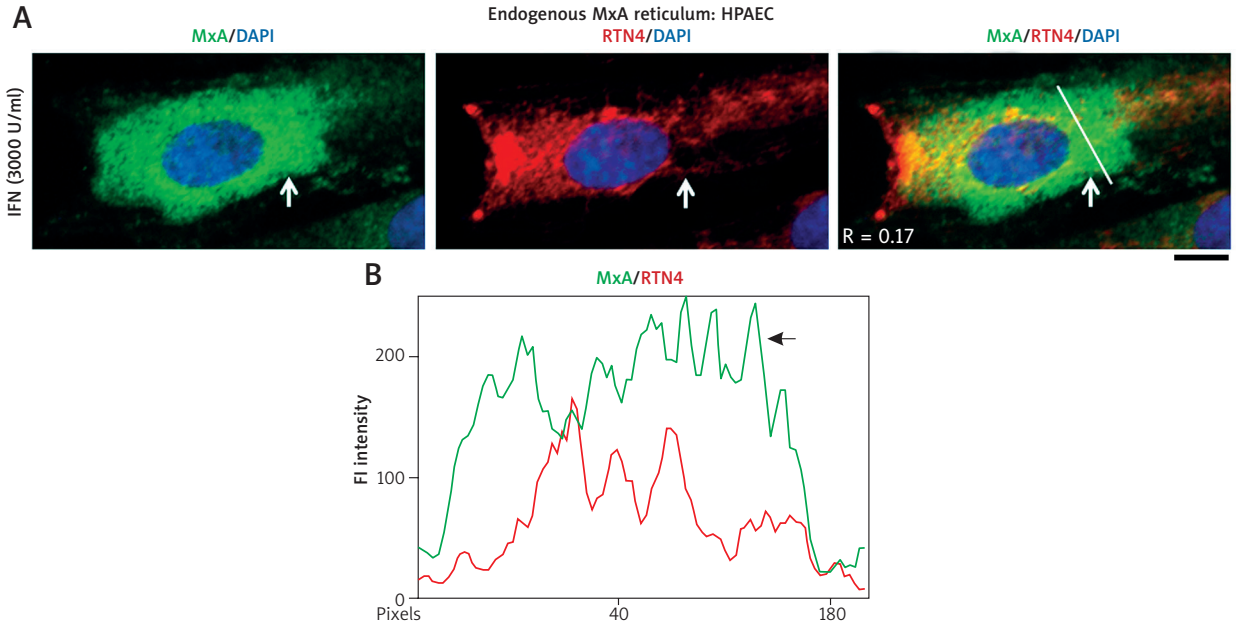

Fig. 3. IFN-α-induced endogenous MxA in HPAECs was in cytoplasmic structures distinct from the RTN4-based ER. HPAEC cultures (in 35 mm plates) were exposed overnight to IFN-α2a (3,000 IU/ml) as in ref. 21, fixed and MxA localization compared to that of RTN4 using sequential double-label immunofluorescence methods. While the majority of cells showed MxA in small endosomes (as in Fig. 1 in ref. 21), 10–25% of cells in a given culture showed MxA in vesicular or reticulotubular structures. From within the latter subset, three representative cells with different phenotypes are shown in Figs. 3A, 4A and 4C. Panel A and the line scan in Panel B (corresponding to the white line in the merged image in Panel A) show a cell with MxA in a fine reticular distribution distinct from RTN4-ER (*R* = 0.17). Arrow in Panel A points to a particularly distinctive area; also see arrow in Panel B for further validating the distinction between MxA and RTN4. Scale bar = 10 μm

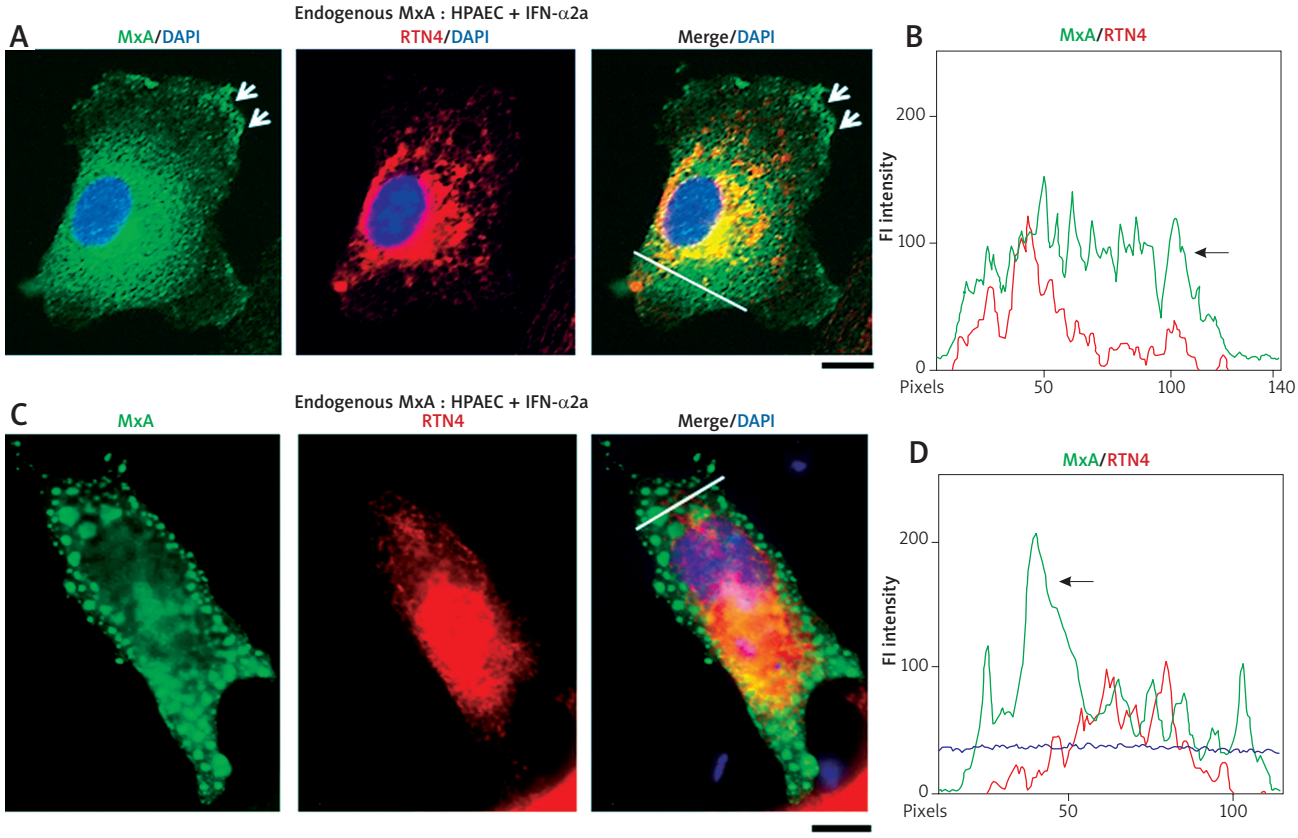

Fig. 4. IFN-α-induced endogenous MxA in HPAECs was also at the plasma membrane and in larger globular structures. Panels A and C show IFN-treated HPAEC cells from the experiment in Fig. 3 which showed the induced endogenous MxA at the plasma membrane (arrows in Panel **A)** and in a fine reticular meshwork in the cytoplasm. The latter was distinct from the RTN4-ER (arrow in the line scan in Panel **B)**. Panels C and D show an IFN-α-treated HPAEC cell with MxA in globular structures throughout the cytoplasm which are RTN4-negative. The line scan in Panel D confirms the distinctness of the MxA structures (arrow in line scan in Panel **D)**. Scale bars = 10 μm. *R* values correspond to the Pearson's correlation coefficients (after automatic Costes' thresholding)

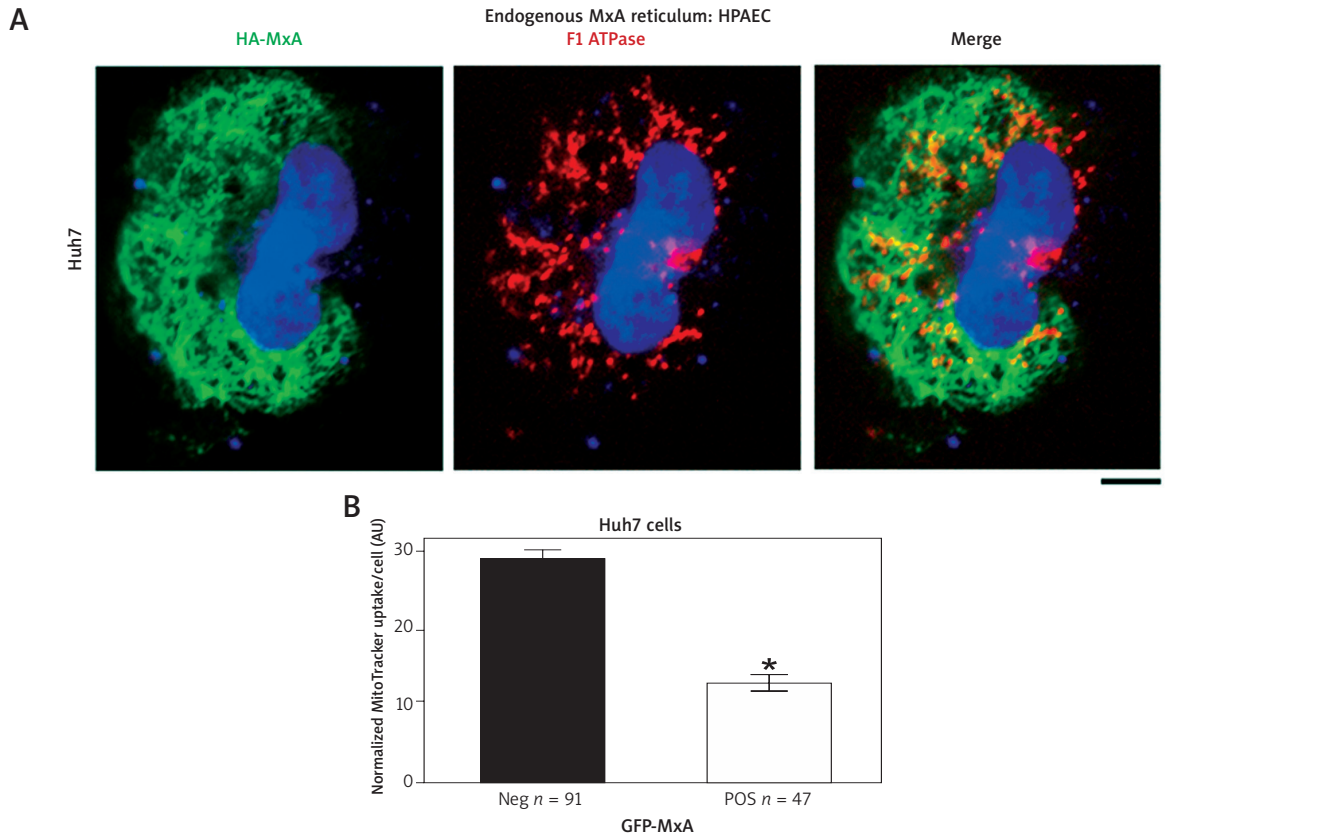

Fig. 5. MxA reticulum in Huh7 cells was distinct from but affected mitochondrial function. Panel A. Huh7 cells were transfected with the HA-MxA expression vector, fixed 2 days later, permeabilized using Triton X-100 (0.5% in PBS, 5 min), and evaluated for localization of HA-MxA (using an anti-MxA pAb) and mitochondria (using an anti-F1-ATPase mAb). Scale bar = 10 µm. An $R = 0.32$ suggests that while the two were distinct, they were in close vicinity. Panel B. Huh7 cells were transfected with the GFP-MxA vector, and MitoTracker uptake evaluated 2 days later (5 nM for 15 min) in GFP-negative and GFP-positive cells. *$p < 0.05$ using Student's *t*-test

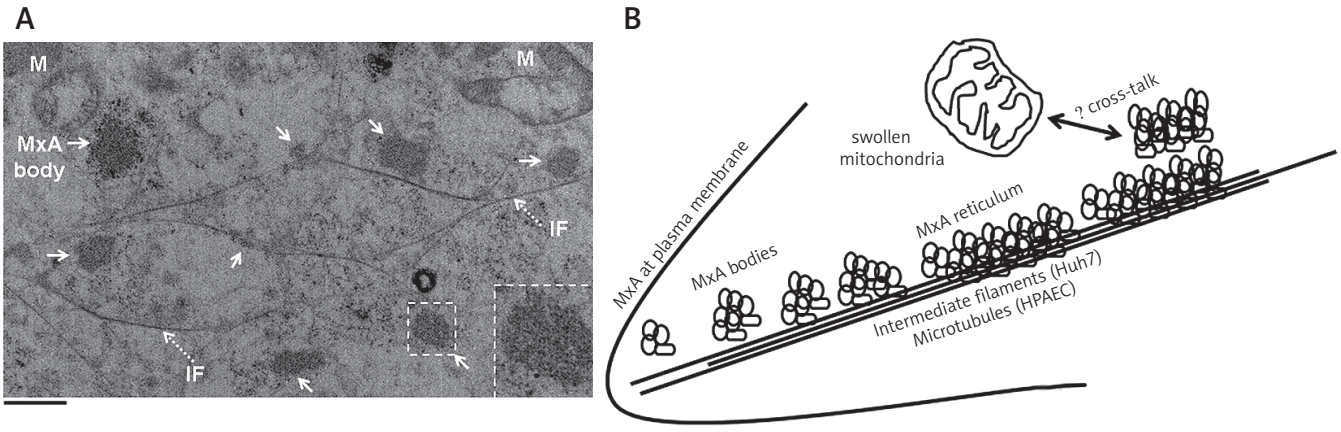

Fig. 6. Structure of GFP-MxA bodies in the cytoplasm of Huh7 cells by CLEM and an interpretative schematic. Panel A. Huh7 cells plated sparsely on a gridded coverslip 35 mm plate were transfected with the GFP-MxA expression vector and fixed with paraformaldehyde two days later. The cells were first imaged by fluorescence light microscopy, and location of GFP-positive cells identified. The cultures were processed further for thin-section EM focusing on the GFP-positive cells. Panel A illustrates thin-section EM of a GFP-positive cell showing MxA "bodies" (solid arrows) associated with intermediate filaments (dotted arrows, and "IF") as well as swollen mitochondria ("M"). Additional experiments confirm that the MxA-bodies correspond to GFP fluorescence (data not shown). Inset show one such "MxA body" at higher magnification. Scale bar = 1 µm. Panel B. Interpretive schematic of MxA at the plasma membrane and in variably-sized clusters of individual MxA vesiculo-tubular elements some of which associated with and stretched out alongside cytoskeletal elements (intermediate filaments and/or microtubules). The mechanism for cross-talk between MxA structures and mitochondria (leading to swelling and reduced function) remains open to further exploration

aligned themselves along intermediate filaments (dotted arrows and "IF" in Fig. 6A). Moreover, the thin-section EM images show swollen mitochondria ("M" in Fig. 6A) in the vicinity of MxA structures i.e. in GFP-MxA expressing cells consistent with the reduced MitoTracker uptake data in such cells summarized in Figure 5B. These data suggest the occurrence of cross-talk between cytoplasmic MxA structures and mitochondria.

Discussion

An aim of this study was to characterize the association of IFN-α-induced MxA with cytoplasmic structures in human Huh7 liver cancer cells and primary endothelial cells. Specifically, we re-evaluated the long-standing claim that MxA associated with the smooth ER [14–16, 24] using double-label immunofluorescence and the ER structural protein RTN4 as a marker for smooth ER tubules. We discovered that IFN-α-induced MxA associated with endosome-like and reticular cytoplasmic structures clearly distinct from the standard ER. The present observations pertaining to endogenous MxA complement our previous studies showing that HA-MxA or GFP-MxA expressed in these cells following transient transfection of respective vectors also associated with endosome-like and reticular structures distinct from the RTN4-based ER [21–23]. Thin-section EM studies of GFP-MxA expressing Huh7 cells showed that GFP-MxA formed variably sized clusters of vesiculo-tubular elements without a limiting membrane (Fig. 6B). We believe that these MxA bodies represent the endosome-like motile MxA structures observed by light microscopy [21–23]. Many of these "MxA bodies" lined up alongside cytoskeletal elements in the cytoplasm likely giving rise to a filamentous/reticular appearance when viewed using diffraction-limited light microscopy (Fig. 6B). While the MxA "reticulum" was distinct from mitochondria, we observed reduced mitochondrial function and swollen mitochondria in GFP-MxA expressing cells. These data suggest novel mechanisms of cross-talk between MxA bodies in the cytoplasm and mitochondria that might account for the increased anti-tumoral efficacy of IFN-α together with ligands that activate the TLR, MAVS or STING signaling pathways.

Human MxA is a cytoplasmic protein which has a broad-spectrum antiviral activity against diverse RNA viruses including influenza, thogotavirus, flaviviruses, hepatitis C virus and HIV [14–16]. The GTPase activity is required for its antiviral effects [14–16]. Many of the viruses inhibited by MxA replicate and/or mature in the cytoplasm in association with cytoplasmic membranes [29, 30]. Although, previous studies have presumed that MxA can sequester proteins critical for viral replication in specialized membrane-limited compartments in the cytoplasm as one of the mechanisms of generating an antiviral effect [14–16], there has been no clear evidence by thin-section EM that these MxA/viral protein structures have an external enveloping membrane [14–16]. In the present CLEM studies, the MxA structures were observed to be devoid on an external limiting membrane, but appeared to possess an internal vesiculo-tubular architecture and an electron dense matrix. How these cytoplasmic MxA structures participate in mechanisms leading to an antiviral effect remains to be explored.

It has long been established that IFNs decrease cancer cell proliferation, cell motility and invasiveness [2–6, 17]. In characterizing the effects of an IFN-inducible protein such as MxA in cancer cells and models of cancer metastasis, Mushinski *et al.* discovered that exogenously expressed wild-type MxA interacted with α-tubulin and inhibited the motility and invasiveness of PC3M prostate cancer cells, including their hepatic metastasis [17]. The GTPase-defective mutants of MxA did not have this activity [17]. Brown *et al.* [18] later reported that deletion of MxA was inversely associated with prostate cancer and that MxA regulated the cell cycle, invasiveness and docetaxel-induced apoptosis in prostate cancer cells More recently, working in Huh7 hepatoma cells, Shi *et al.* [20] observed that transient exogenous expression of MxA reduced hepatitis C virus replication, stimulated IFN-α and β production as well as the expression of several IFN-pathway genes, suggesting to us the cross-activation of the STING pathway by MxA. The combinatorial cross-talk between cytoplasmic MxA structures in IFN-α-treated cancer cells and other cytoplasmic organelles appears to be a fertile avenue of basic science exploration in the furtherance of improved immunotherapy of cancer.

Acknowledgement

This study was supported, in part, by Bridge Funding from the New York Medical College.

The authors declare no conflict of interest.

References

1. Sehgal PB, Pfeffer LM, Tamm I. Interferon and its Inducers. Handbook of Experimental Pharmacology 1982; 61: 203-311.
2. Muller L, Aigner P, Stoiber D. Type I interferons and natural killer cell regulation in cancer. Front Immunol 2017; 8: 304.
3. Kiladjian IJ, Giraudier S, Cassinet B. Interfeon-α for the therapy of myeloproliferative neoplasms: targeting the malignant clone. Leukemia 2016; 30: 776-781.
4. Talpaz M, Mercer J, Hehlmann R. The interferon-α revival in CML. Ann Hematol 2015; 94 Suppl 2: S195-207.
5. Gajewski TF, Corrales L, New perspectives on Type I interferons in cancer. Cytokine Growth Factor Rev 2015; 26: 175-178.
6. Haji Abdolvahale M, Mofred MR, Schellekens H. Interfeon-β: from molecular level to therapeutic effects. Int Rev Cell Mol Biol 2016; 326: 343-372.
7. Li Y, Wilson HL, Kiss-Toth E. Regulating STING in health and disease. J Inflammation 2017; 14: 11.
8. Wu J, Chen ZJ. Innate immune sensing and signaling of cytosolic nucleic acids. Ann Rev Immunol 2014; 32: 461-488.
9. Barber GN. STING: infection, inflammation and cancer. Nat Rev Immunol 2015; 15: 760-770.
10. Zevini A, Olagnier D, Hiscott J. Crosstalk between cytoplasmic RIG-1 and STING sensing pathways. Trends in Immunol 2017; 38: 194-205.
11. Liu S, Cai X, Wu J, et al. Phosphorylation of innate immune adaptor proteins MAVS, STING, and TRIF induces IRF3 activation. Science 2015; 347: 1217.

12. Corrales L, McWhirter SM, Dubensky TW, Gajewski TF. The host STING pathway at the interface of cancer and immunity. J Clin Invest 2016; 126: 2404-2411.
13. Kalinski P. Combinatorial adjuvants and dendritic cell therapies sensitize "cold" tumors to checkpoint blockade. 10th Anniversary International Conference of Contemporary Oncology, Progress in Cancer Research and Therapy, Contemporary Oncology, March 21-23, Poznan, Poland (abstract).
14. Haller O, Kochs G. Interferon-induced mx proteins: dynamin-like GTPases with antiviral activity. Traffic 2002; 3: 710-717.
15. Haller O, Staeheli P, Kochs G. Interferon-induced Mx proteins in antiviral host defense. Biochimie 2007; 89: 812-818.
16. Haller O, Staeheli P, Schwemmle M, Kochs G. Mx GTPases: dynamin-like antiviral machines of innate immunity. Trends Microbiol 2015; 23: 154-163.
17. Mushinski JF, Nguyen P, Stevens LM, et al. Inhibition of tumor cell motility by the interferon-inducible GTPase MxA. J Biol Chem 2009; 284: 15206-15214.
18. Brown SG, Knowell AE, Hunt A, Patel D, Bhisle S, Choudhary J. Interferon inducible antiviral MxA is inversely associated with prostate cancer and regulates cell cycle, invasion and Docetaxel-induced apoptosis. Prostate 2015; 75: 266-279.
19. Hu JL, Hua YJ, Chen Y, Yu B, Gao S. Structural analysis of tumor-related single amino acid mutations in human MxA protein. Chin J Cancer 2015; 34; 583-593.
20. Shi X, Jiao B, Chen Y, Li S, Chen L. MxA is a positive regulator of type I IFN signaling in HCV infection. J Med Virol 2017; 89: 2173-2180.
21. Yuan H, Sehgal PB. MxA Is a Novel Regulator of Endosome-Associated Transcriptional Signaling by Bone Morphogenetic Proteins 4 and 9 (BMP4 and BMP9). PLoS One 2016; 11: e0166382.
22. Sehgal, PB, Yuan H, Davis D, Petzold C, Dancel-Manning K, Liang FX. MxA reticulum is a novel organelle distinct from the standard reticulon-4-based endoplasmic reticulum. Mol Biol Cell 2016; 26: 504.
23. Yuan H, Davis D, Petzold C, Dancel-Manning K, Liang FX, Sehgal PB. Live-cell imaging of GFP-MxA – endosomes and GFP-MxA – reticulum in human Huh7 cells. Mol Biol Cell 2017; 27: 3727 (#2365).
24. Stertz S, Reichelt M, Krijnse-Locker J, Mackenzie J, Simpson JC, Haller O, Kochs G. Interferon-induced, antiviral human MxA protein localizes to a distinct subcompartment of the smooth endoplasmic reticulum. J Interferon Cytokine Res 2006; 26: 650-660.
25. Blight KJ, McKeating JA, Rice CM. Highly permissive cell lines for subgenomic and genomic hepatitis C virus RNA replication. J Virol 2002; 76: 13001-13014.
26. Wisskirchen C, Ludersdorfer TH, Muller DA, Moritz E, Pavlovic J. Interferon-induced antiviral protein MxA interacts with the cellular RNA helicases UAP56 and URH49. J Biol Chem 2011; 286: 34743-34751.
27. Nigg PE, Pavlovic J. Oligomerization and GTP-binding Requirements of MxA for Viral Target Recognition and Antiviral Activity against Influenza A Virus. J Biol Chem 2015; 290: 29893-29906.
28. Dunn KW, Kamocka MM, McDonald JH. A practical guide to evaluating colocalization in biological microscopy. Am J Physiol Cell Physiol 2011; 300: C723-C742.
29. Caliguiri LA, Tamm I. Mebrnanous structures associated with translation and transcription of poliovirus RNA. Science 1969; 166: 885-886.
30. Ravindran MS, Bagchi P, Cunningham CN, Tsai B. Opportunistic intruders: how viruses orchestrate ER functions to infect cells. Nat Rev Microbiol 2016; 14: 407-420.

Address for correspondence

Pravin B. Sehgal
Department of Cell Biology & Anatomy
New York Medical College
Valhalla, NY 10595, USA
e-mail: pravin_sehgal@nymc.edu

Submitted: 16.04.2018
Accepted: 17.04.2018